Infrared properties of $CsGe(Br_xCl_{1-x})_3$, nonlinear optical rhombohedral semiconductor

2007 J. Phys.: Condens. Matter 19 476209

(http://iopscience.iop.org/0953-8984/19/47/476209)

J. Phys.: Condens. Matter **19** (2007) 476209 (10pp) doi:10.1088/0953-8984/19/47/476209

Infrared properties of $CsGe(Br_xCl_{1-x})_3$, nonlinear optical rhombohedral semiconductor

Zhi-Guang Lin[1], **Li-Chuan Tang**[2] **and Chang-Pin Chou**[1,3]

[1] Department of Mechanical Engineering, National Chiao Tung University, Hsinchu 305, Taiwan, Republic of China
[2] Department of Electrical Engineering, Chung-Cheng Institute of Technology, National Defense University, Taoyuan 353, Taiwan, Republic of China

E-mail: zglin.me91g@nctu.edu.tw

Received 16 June 2007, in final form 9 October 2007
Published 31 October 2007
Online at stacks.iop.org/JPhysCM/19/476209

Abstract

Innovative infrared nonlinear optical crystals $CsGe(Br_xCl_{1-x})_3$ were synthesized. From their powder x-ray diffraction patterns, these crystals were characterized as rhombohedral structure with ($R3m$, No 160) space group symmetry. The energy gap decreased from about 3.43 to 2.38 eV as the substitutional ratio, x, changed from zero to unity. Moreover, the powder second-harmonic generation (PSHG) measurement of $CsGeBr_3$ showed that its nonlinear optical efficiency is 9.64 times larger than that of rhombohedral $CsGeCl_3$ and 28.29 times larger than that of KH_2PO_4 (KDP), and most important of all, that $CsGe(Br_xCl_{1-x})_3$ is phase matchable. So the optical nonlinearity is approximately inversely proportional to the cube of the energy gap. The infrared transparent spectrum of rhombohedral $CsGe(Br_xCl_{1-x})_3$ was extended to more than 30 μm, which shows the potential in the realm of nonlinear optics and can be applied to the infrared region.

(Some figures in this article are in colour only in the electronic version)

1. Introduction

Second-order nonlinear optical (NLO) materials have played a key role in such optical fields as laser frequency conversion and optical parametric oscillation/amplification (OPO/OPA) [1, 2]. For inorganic second-order NLO materials, several crystals used in ultraviolet (UV) and visible regions have been proposed in the past two decades, such as KH_2PO_4 (KDP), $KTiOPO_4$ (KTP), β-BaB_2O_4 (BBO) and LiB_3O_5 (LBO). But in the infrared (IR) region the current materials, such as $AgGaSe_2$, $ZnGeP_2$, are not good enough for applications mainly due to their low laser damage threshold, as their band-gaps were smaller than 1.5 eV. So the search for new NLO

[3] Author to whom any correspondence should be addressed.

crystals with excellent properties, especially a high damage threshold, has become one of the key research areas in NLO material science and laser technology [3].

Crystals with a pyramidal basis are known to exhibit a fairly large optical nonlinearity. A pyramidal basis in a unit cell contains one tetrahedron with one cation and three anions located at the vertices, such as the pyramidal basis $-GeCl_3$ [4, 5] in the $CsGeCl_3$ (CGC) crystal. Ternary halides are found to be potential materials for use in nonlinear optical applications [6] and are expected to be transparent in the mid-infrared region (with the exception of the fluorides) [7]. Furthermore, CGC's damage threshold reaches 200 MW cm^{-2} [8]. The optical damage threshold and the transparent range of materials are related to the magnitude of the energy gap, while the optical nonlinearity is inversely proportional to the cubic power of the energy gap [9]. To meet the demand from specific applications, the linear and NLO properties of $CsGe(Br_xCl_{1-x})_3$ can be adjusted by varying the alloy composition. In this paper, the synthetic method of crystals and measurements of the optical properties in each composition are reported. Nonlinear coefficients of $CsGe(Br_xCl_{1-x})_3$, $x = 0, 1/4, 2/4, 3/4, 1$, are also determined to reveal the potential of these crystals in NLO applications.

2. Synthesis and measurement

2.1. Synthesis

The procedure of synthesis is illustrated in figure 1, which was modified from the work done by Gu *et al* [10, 8, 11]. Christensen and Tananaev *et al* [4, 12] used different synthesis methods, but their methods seemed complex and the productivity was poor. In this study, H_3PO_2 (50%) was loaded with HBr (48%), HCl (37%), and GeO_2 (99.999%) into a 250 ml beaker, and then heated to 95 °C. The solution was vigorously mixed for 5 h and then cooled to room temperature. After removing the precipitate, CsBr (99.9%) was added and the temperature raised to boiling, then the mixture was naturally cooled to room temperature again. A light yellow precipitate was formed. The reaction equations were listed as follows:

$$H_3PO_2 + 6xHBr + 6(1-x)HCl + 2GeO_2 = H_3PO_4 + 2HGe(Br_xCl_{1-x})_3 + 2H_2O \quad (1)$$

then

$$HGe(Br_xCl_{1-x})_3 + CsBr = CsGe(Br_xCl_{1-x})_3 \downarrow + HBr. \quad (2)$$

Recrystallization was done by mixing the precipitate with 1:1 concentrated HX and alcohol solution to give the yellow crystals $CsGe(Br_xCl_{1-x})_3$. To avoid residue of the precursor, we repeat this procedure seven times. Then, the crystals were dried at 85 °C for 48 h under vacuum to prevent the influence of deliquescence. The color of precipitated product varied from yellow to white as soon as the substitutional ratio, x, changed from unity to zero.

2.2. Physical measurements

The $CsGe(Br_xCl_{1-x})_3$ crystals were synthesized and sieved into different particle sizes in order to measure and analyze their structural and optical properties. The crystal structures were observed using an x-ray diffractometer. The composition of all samples was measured by electron-probe x-ray microanalysis (EPMA). The optical transmission spectra in the infrared region was determined by a Fourier-transform infrared spectrometer (FTIR) while the absorption edge was measured by a UV–vis spectrometer. Linear optical properties were measured by an ellipsometer. Nonlinear optical properties were determined by powder second-harmonic generation measurements.

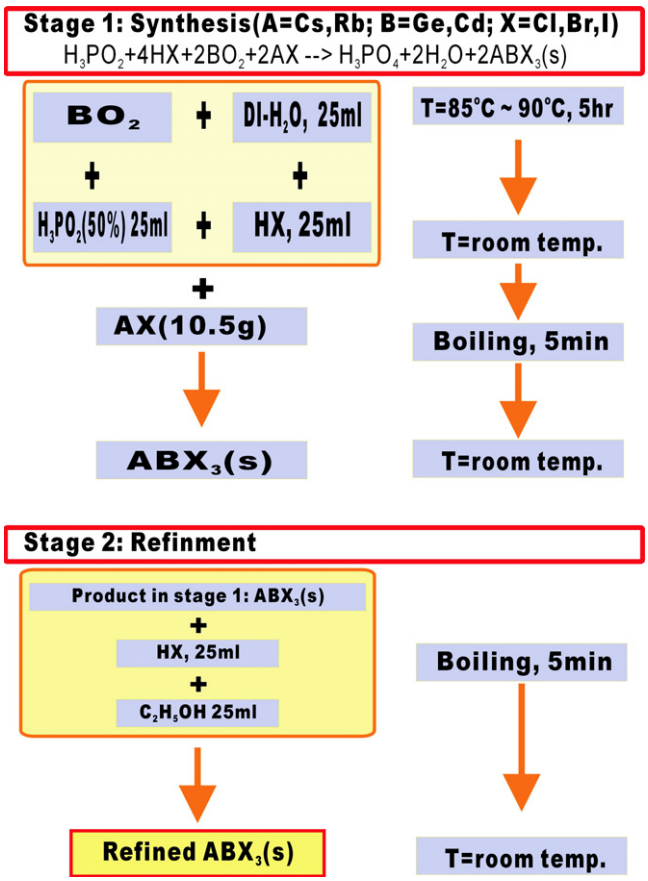

Figure 1. The synthesis procedure of rhombohedral nonlinear optical crystals $CsGe(Br_xCl_{1-x})_3$.

3. Results and discussion

3.1. Composition and structural properties

The results of EPMA measurement (table 1) reveal that those samples possess a Cs to Ge ratio of almost 1:1 and confirm qualitatively that chlorine atoms were successfully doped in the $CsGeBr_3$ crystal. Though there are still some impurities, they are all smaller than 1% ($O_{max} \leqslant 0.47\%$, $P_{max} \leqslant 0.58\%$).

XRD measurement, which was obtained at room temperature by means of Cu Kα radiation with Siemens D5000 equipment, was employed to determine the structural parameters of all the $CsGe(Br_xCl_{1-x})_3$ crystals. The results are shown in figure 2: the substitution-related diffraction peaks shifted gradually with substitute composition. Moreover, the measured pattern was indexed and analyzed by a non-profit program *PowderCell* [13], which was developed by Kraus and Nolze. The structural parameters of $CsGe(Br_xCl_{1-x})_3$ were compared with both $CsGeCl_3$ and $CsGeBr_3$, which were reported in JCPDS [14–17, 7]. There were certain stronger diffraction peaks observed at $2\theta = 31.76°$, $27.66°$, $26.86°$, $22.60°$, $22.10°$, and $15.76°$ in $CsGeBr_3$. These diffraction patterns were compared with JCPDS and were indexed with (200), $(1\bar{1}1)$, (111), $(1\bar{1}0)$, (110), and (100) planes, respectively. The result also confirmed that

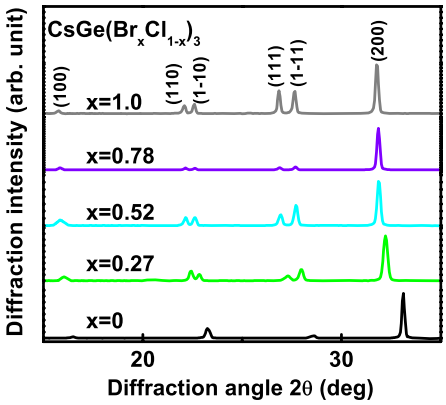

Figure 2. The x-ray powder diffraction results for nonlinear optical crystals $CsGe(Br_xCl_{1-x})_3$.

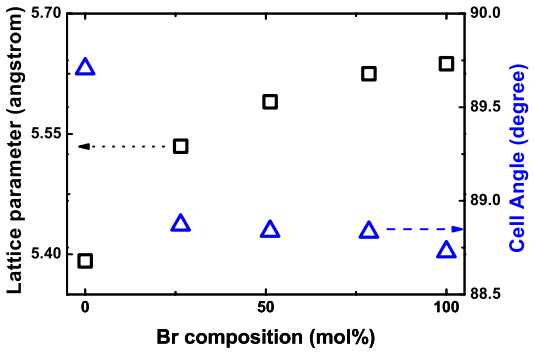

Figure 3. The structural parameters for nonlinear optical crystals $CsGe(Br_xCl_{1-x})_3$.

Table 1. The composition of the rhombohedral NLO crystals $CsGe(Br_xCl_{1-x})_3$ ($x = 0, 1/4, 2/4, 3/4, 1$) from EPMA measurements.

	x				
	0/4	1/4	2/4	3/4	4/4
Cs	20.56	20.16	20.57	20.20	20.32
Ge	20.66	20.70	20.61	20.26	20.51
Br	0	15.26	30.15	44.89	58.17
Cl	58.04	43.15	27.74	14.19	0
O	0.45	0.47	0.35	0.34	0.46
P	0.29	0.26	0.58	0.12	0.54

$CsGe(Br_xCl_{1-x})_3$ crystallized in the non-centrosymmetric rhombohedral space group $R3m$. Moreover, the splitting differences between $(1\bar{1}1)$ with (111) and $(1\bar{1}0)$ with (110) get closer as the containment of Br decreases in $CsGe(Br_xCl_{1-x})_3$. The cell parameters, which were refined from powder XRD in figure 3, showed that the lattice constant became larger as Br increased while the cell angle became smaller as Br increased. Therefore, the structural distortion of $CsGe(Br_xCl_{1-x})_3$ ($R3m$) will increase as Br increases.

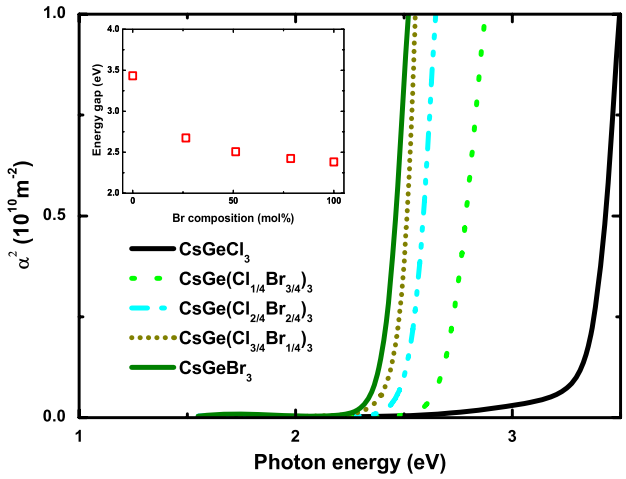

Figure 4. Absorption coefficient near the band edge of CsGe(Br_xCl_{1-x})$_3$ plotted in coordinates α^2 and $h\nu$. The inset shows the Br composition dependence of the energy gap obtained.

3.2. Optical transparent properties

For the absorption edge measurements, thin plates (≈500 μm) of CsGe(Br_xCl_{1-x})$_3$ were used. In figure 4, the absorption spectrum measured at room temperature in the UV–visible light range is shown. The recorded curves can be approximated with straight lines in the coordinates α^2 and $h\nu$, where α is the absorption coefficient and $h\nu$ is the photon energy. The straight line approximation is applied to the rapidly increasing portions of the curves in figure 4. Thus, the fundamental absorption edge is described by the $\alpha = A(h\nu - E_g)^{1/2}$ dependence, where A is a constant and the approximate band-gap E_g can be determined from the cross points of the straight lines with the abscissa. This dependence corresponds to direct allowed electronic transitions [18]. In the inset of figure 4, the energy gap values are plotted versus Br composition. The absorption edge is found to decrease from about 3.43 to 2.38 eV as the substitutional ratio, x, changes from zero to unity.

Infrared spectra were recorded on the spectrometer (Bomem, DA8.3) in the range from 120 to 4000 cm^{-1} with the specimens pressed into thin plates (≈500 μm). From figure 5, FTIR measurements showed that the long wavelength limit of the transparent range of the crystals exhibited a similar dependence on substitute composition. The crystal $CsGeCl_3$ had an infrared cut-off wavelength at approximately 30 μm, which was shorter than the cut-off value of $CsGeBr_3$ (approximately 47 μm). The infrared absorption edge of CsGe(Br_xCl_{1-x})$_3$ with $x = 1/4, 2/4, 3/4$ lay approximately from 32 to 37 μm. This result agreed with the effective-mass concept that the infrared transparency range of CGB is expected to be wider than that of CGC owing to the fact that the Br atom is heavier than Cl. The results of FTIR at room temperature are presented in figure 6. The transmission range of the crystals extends wider as Br increases. The longest infrared transparency wavelength is usually limited by the phonon absorption of the crystal. Moreover, the absorption edge is limited by the energy band-gap of the crystal.

3.3. Second-order nonlinear optical measurements

Powder SHG measurements were performed on a modified Kurtz-NLO [19] system using 1260 nm light. Since the SHG efficiency of powders has been shown to depend strongly on

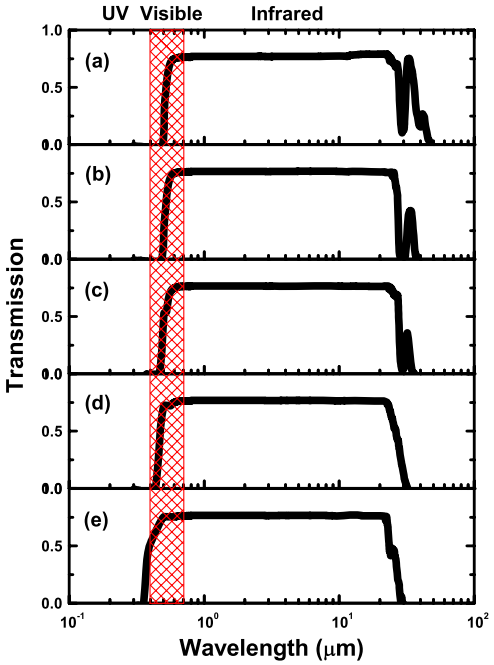

Figure 5. The full transmission range of the nonlinear optical crystals $CsGe(Br_xCl_{1-x})_3$ (a) $x = 1$, (b) $x = 3/4$, (c) $x = 2/4$, (d) $x = 1/4$, (e) $x = 0$.

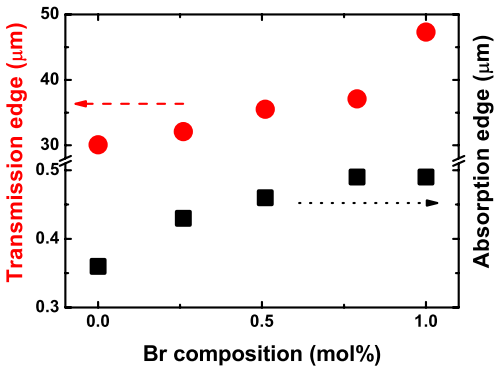

Figure 6. The transmission edge and absorption edge of nonlinear optical crystals $CsGe(Br_xCl_{1-x})_3$.

particle size [19, 20], polycrystalline $CsGe(Br_xCl_{1-x})_3$ was ground and sieved (Newark Wire Cloth Company) into six distinct particle-size ranges, 19–37 μm, 37–74 μm, 74–105 μm, 105–210 μm, 210–420 μm and 420–840 μm (see figure 7). To make relevant comparison with known SHG materials, crystalline KDP was also ground and sieved into the same particle-size ranges. All of the powders were placed in separate capillary tubes. We filled the capillary tube as full as possible with $CsGe(Br_xCl_{1-x})_3$ powders. But it was averaged slightly loosely in the two extremities. Though the powder was suspended in air in the two extremities, we chose the compact part when performing the nonlinear optical characterization. The SHG radiation (630 nm) was collected in transmission and detected by a photomultiplier tube (Oriel

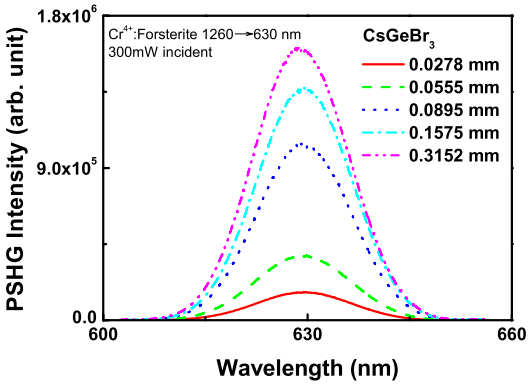

Figure 7. The powder second-harmonic generation results for rhombohedral nonlinear optical crystals $CsGeBr_3$.

Table 2. The ellipsometry measurements of the rhombohedral NLO crystals $CsGe(Br_xCl_{1-x})_3$ ($x = 0, 1/4, 2/4, 3/4, 1$).

	x				
$CsGe(Br_xCl_{1-x})_3$	0.00	0.27	0.52	0.78	1.00
$\alpha_{630\,nm}$ (1/mm)	1.49	3.80	5.26	4.45	8.88
$n_{630\,nm}$	1.71	1.89	1.78	1.58	1.63
$n_{1260\,nm}$	1.67	1.86	1.78	1.64	1.68

Instruments). The SHG signal was collected by a data-acquisition (DAQ) interface and was monitored by a personal computer with the analysis program.

If the SHG process was phase matchable and satisfied the type-I phase-matching conditions, the intensity of the SHG response could be written as [21]

$$I_{2\omega}(\bar{r},\theta) = \frac{128\pi^5 I_\omega^2}{n_\omega^2 n_{2\omega}\lambda_{2\omega}^2 c} L\bar{r}\langle d_{\text{eff}}^2\rangle \frac{\sin^2\left[\frac{\pi}{2}\frac{\bar{r}}{\bar{l}_{\text{pm}}}(\theta-\theta_{\text{pm}})\right]}{\left[\frac{\pi}{2}\frac{\bar{r}}{\bar{l}_{\text{pm}}}(\theta-\theta_{\text{pm}})\right]}, \tag{3}$$

where $\bar{l}_{\text{pm}} = \lambda/[4|\Delta n_{B,2\omega}|\sin 2\theta_{\text{pm}}]$, and θ_{pm} is the phase-matching angle. Here $\Delta n_{B,2\omega} = n_{E,2\omega} - n_{O,2\omega}$ denotes the birefringence of the material at the second-harmonic wavelength. In the event that $\bar{r} \gg \bar{l}_{\text{pm}}$ or $\bar{r} \ll \bar{l}_{\text{pm}}$, equation (3) could be simplified to

$$I_{2\omega} \to \left\{ \begin{array}{l} [(256\pi^4 I_\omega^2)/(n_\omega^2 n_{2\omega}\lambda_{2\omega}^2 c)]L\bar{l}_{\text{pm}}\langle d_{\text{eff}}^2\rangle, \longleftarrow \bar{r} \gg \bar{l}_{\text{pm}} \\ [(128\pi^5 I_\omega^2)/(n_\omega^2 n_{2\omega}\lambda_{2\omega}^2 c)]L\bar{r}\langle d_{\text{eff}}^2\rangle, \longleftarrow \bar{r} \ll \bar{l}_{\text{pm}} \end{array} \right]. \tag{4}$$

The SHG signals became saturated when the average particle sizes were larger than $\bar{l}_{\text{pm}}$ and independent of the particle size.

Chen *et al* [22] derived a useful empirical formula, which possessed the correct asymptotic forms in equation (4), to depict the overall variation in the second-harmonic intensity with a particle size $\bar{r}$

$$I_{2\omega} = \frac{256\pi^4 I_\omega^2}{n_\omega^2 n_{2\omega}\lambda_{2\omega}^2 c} L\bar{l}_{\text{pm}}\langle d_{\text{eff}}^2\rangle\sqrt{1-\exp[-(\bar{r}/A)^2]} \tag{5}$$

with $A \approx 9\bar{l}_{\text{pm}}$.

Because the absorption coefficient of $CsGeBr_3$ at 630 nm was too large, the saturated PSHG intensity decayed. To modify such a situation, the absorption coefficients (from table 2)

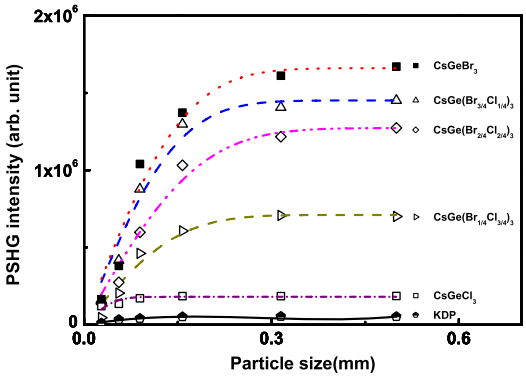

Figure 8. The comparison of integrated powder second-harmonic generation intensity of nonlinear optical crystals KDP and $CsGe(Br_xCl_{1-x})_3$.

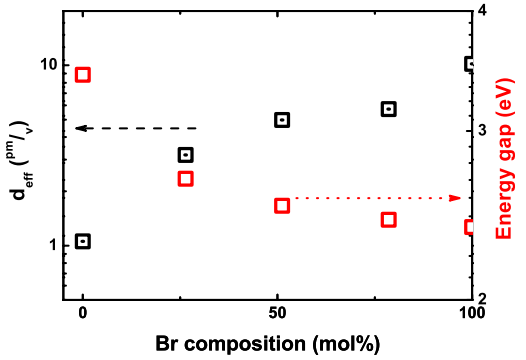

Figure 9. The effective powder second-harmonic generation coefficients of nonlinear optical crystals $CsGe(Br_xCl_{1-x})_3$ and their energy gaps.

were adopted to calculate the real saturated PSHG intensity using $I_{2\omega} = I_{2\omega}^{\text{total}} \exp[-(\alpha)z]$. The square of the effective nonlinearity, $\langle d_{\text{eff}}^2 \rangle$, averaged over the orientation distribution of crystalline powders of $CsGe(Br_xCl_{1-x})_3$, was determined by equation (6) using a reference NLO crystal, e.g. KDP.

$$\langle d_{\text{eff}}^2 \rangle_{\text{CGB}} = \langle d_{\text{eff}}^2 \rangle_{\text{KDP}} \frac{I_{2\omega,\text{CGB}}^{\text{total}} n_{\omega,\text{CGB}}^2 n_{2\omega,\text{CGB}}}{I_{2\omega,\text{KDP}}^{\text{total}} n_{\omega,\text{KDP}}^2 n_{2\omega,\text{KDP}}} \approx \langle d_{\text{eff}}^2 \rangle_{\text{KDP}} \frac{I_{2\omega,\text{CGB}}^{\text{total}} n_{\text{CGB}}^3}{I_{2\omega,\text{KDP}}^{\text{total}} n_{\text{KDP}}^3} \tag{6}$$

when $n \approx n_\omega \approx n_{2\omega}$.

3.4. Nonlinear optical properties

Figure 8 revealed that the SHG efficiencies of $CsGe(Br_xCl_{1-x})_3$ were higher than that of KDP. Moreover, all of them were phase matchable, as was KDP. That is, as the particle size becomes substantially larger than the coherence length of the crystal, the collected SHG intensity does not gain any more and saturates at a certain value. The saturated PSHG intensities were estimated from the transmission signals for various particle sizes, and showed that the SHG responses enhance as Br increases. From table 2 and $d_{\text{KDP}}(= 0.36\ \text{pm V}^{-1})$ [23], d_{eff} values were calculated and are shown in figure 9. The effective PSHG coefficients increased as Br increased. The nonlinearity (see figure 10) of d_{eff}^2/n^3 of $CsGe(Br_xCl_{1-x})_3$ crystals exhibited

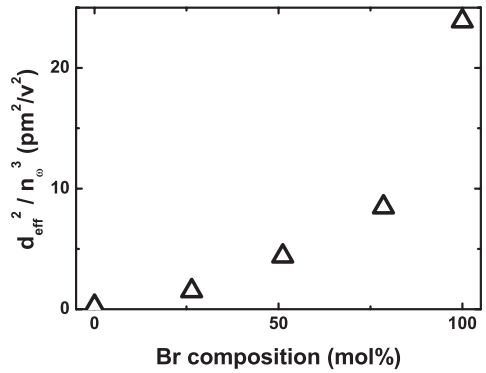

Figure 10. The nonlinearity of d_{eff}^2/n^3 for nonlinear optical crystals $CsGe(Br_xCl_{1-x})_3$.

a similar dependence on substitution composition. There are some reasons for the significant SHG signals of rhombohedral $CsGe(Br_xCl_{1-x})_3$ crystals. First of all, the SHG responses were contributed from the structural distortion and the off-center Ge ion in the unit cell. From the results of XRD, the structural distortion increases as Br increases. Moreover, the cell angle distortion also becomes larger as Br increases. So the position of the B-site cation, Ge, is closer to the cell corner as Br increases. Second, the optical nonlinearity is approximately inversely proportional to the cube of the energy gap [9]. So the energy gap decreased and the NLO susceptibilities increased as the atomic weights of halides increased.

4. Conclusions

The structural and optical properties of rhombohedral NLO crystals, $CsGe(Br_xCl_{1-x})_3$ ($x = 0, 1/4, 2/4, 3/4$, and 1), have been investigated experimentally to reveal the anion substitution effect. Based on the results, the linearly increasing x caused an increase in lattice constant and second-order NLO susceptibility, but a decrease in energy gap. Because the optical damage threshold and the transparent range of materials are related to the magnitude of the energy gap, while the optical nonlinearity is inversely proportional to the cubic power of the energy gap [9], we could modulate the nonlinear susceptibility coefficient, energy gap, laser damage threshold and transparency range of halides at the same time by anion substitution.

Acknowledgment

The authors are indebted for the financial support of the National Science Council of the Republic of China under the grant NSC 95-2112-M-009-042.

References

[1] Burland D M 1994 *Chem. Rev.* **94** 1
[2] Chemla D S and Zyss J (ed) 1987 *Nonlinear Optical Properties of Organic Molecules and Crystals* (Orlando, FL: Academic)
[3] Dmitriev V G, Gurzadyan G G and Nikogosyan D N 1999 *Handbook of Nonlinear Optical Crystals* 3rd edn (Berlin: Springer)
[4] Christensen A N and Rasmussen S E 1965 *Acta Chem. Scand.* **19** 421
[5] Ewbank M D, Cunningham F, Borwick R, Rosker M J and Gunter P 1997 *CLEO'97 Paper* vol CFA7, p 462
[6] Hagemann M and Weber H-J 1996 *Appl. Phys.* A **63** 67

[7] Seo D-K, Gupta N, Whangbo M-H, Hillebrecht H and Thiele G 1998 *Inorg. Chem.* **37** 407
[8] Gu Q, Pan Q, Wu X, Shi W and Fang C 2000 *J. Cryst. Growth* **212** 605–7
[9] Shen Y R 2002 *The Principles of Nonlinear Optics* (New York: Wiley)
[10] Gu Q, Pan Q, Shi W, Sun X and Fang C 2000 *Prog. Cryst. Growth Charact. Mater.* **40** 89–95
[11] Gu Q, Fang C, Shi W, Wu X and Pan Q 2001 *J. Crystal Growth* **225** 501–504
[12] Tananaev I V, Dzhurinskii D F and Mikhailov Y N 1964 *Zh. Neorg. Khim.* **9** 1570–7
[13] Kraus W and Nolze G 1996 *J. Appl. Cryst.* **29** 301–3
[14] Schwarz U, Hillebrecht H, Kaupp M, Syassen K, von Schnering H-G and Thiele G 1995 *J. Solid State Chem.* **118** 20–7
[15] Schwarz U, Wagner F, Syassen K and Hillebrecht H 1996 *Phys. Rev.* B **53** 12545
[16] Thiele G, Rotter H W and Schmidt K D 1987 *Z. Anorg. Allg. Chem.* **545** 148
[17] Thiele G, Rotter H W and Schmidt K D 1988 *Z. Anorg. Allg. Chem.* **559** 7–16
[18] Pankove J I 1971 *Optical Processes in Semiconductors* (Englewood Cliffs, NJ: Prentice-Hall)
[19] Kurtz S K and Perry T T 1968 *J. Appl. Phys.* **39** 3798–813
[20] Dougherty J P and Kurtz S K 1976 *J. Appl. Crystallogr.* **9** 145–58
[21] Prasad P N and Williams D J 1991 *Introduction to Nonlinear Optical Effects in Molecules and Polymers* (New York: Wiley) chapter 6
[22] Chen W K, Cheng C M, Huang J Y, Hsieh W F and Tseng T Y 2000 *J. Phys. Chem. Solids* **61** 969–77
[23] Tang L C, Huang J Y, Chang C S, Lee M H and Liu L Q 2005 *J. Phys.: Condens. Matter* **17** 7275